

# Visual Timelines of Police Encounters in Body-Worn Camera Footage: Operational Context and Activity Cataloging for Training and Analysis in OpenBWC

Angela Srbnovska  
Department of Computer Science  
Rochester Institute of Technology  
Rochester, NY, USA  
as2179@rit.edu

Christopher Homan  
Department of Computer Science  
Rochester Institute of Technology  
Rochester, NY, USA  
cmhvc@rit.edu

Adrian Martin  
Office of Business Intelligence  
Rochester Police Department  
Rochester, NY, USA  
Adrian.Martin@CityofRochester.gov

Ernest Fokoué  
School of Mathematics and Statistics  
Rochester Institute of Technology  
Rochester, NY, USA  
epfeqa@rit.edu

**Abstract**—Law enforcement agencies are accumulating vast amounts of body-worn camera (BWC) footage. However, this remains operationally opaque. That is, analysts and trainers still have to invest considerable time watching full-length videos to pinpoint the start of key encounters and identify the points where activity shifts to something more physically intense. We present an approach to process BWC video into a time-aligned sequence of fixed-length 10-second windows, processed and labeled using a privacy-conscious protocol. Each window is labeled with two dimensions of information: (i) the operational context of the window and (ii) the level of motion intensity within the window, with low-evidence labels for windows for which insufficient evidence exists due to darkness, blur or occlusion. We train models to classify windows based on these two axes using frames sampled from each window encoded using CLIP model and aggregated into a window-level representation. We extract dense optical flow statistics for each window to capture motion intensity. On test windows the best context model achieves 78.75% accuracy, and the best-accuracy activity model achieves 88.33%. We also included integrity audits to show the results and how the visual timeline representations support faster incident review and make the officer training workflow more practical.

**Index Terms**—Body-worn cameras, human-in-the-loop, temporal windowing, privacy-aware analytics

## I. INTRODUCTION

Police departments have adopted body-worn cameras (BWCs) more over the past decade mainly as a way to capture video of officer-community interactions. As these systems have become more widespread, police agencies now maintain growing archives of BWC video, where individual events can extend from tens of minutes to over an hour. Even when a reviewer has a clear sense of the kind of event they are looking for, the standard approach still often requires watching footage in real time. Reviewers may be trying to answer questions such as:

“When does the officer first enter a residence and when does a foot pursuit begin?”

“How do police encounters change over time?”

“Which segments show high activity motion?”

For these reasons, we design a time-aligned structure that is easy to audit so that we can do systematic reviews on a large scale. In particular, we model two signals:

- 1) **Operational context:** a coarse scene state capturing the encounter setting, which we derive from appearance and layout statistics. We model context as a discrete label that typically evolves in long temporal runs.
- 2) **Motion intensity:** a window-level kinematic regime summarizing the distribution of apparent motion over time. We summarize motion intensity using interpretable motion statistics.

We develop this project within the OpenBWC<sup>1</sup> collaboration that includes the Rochester Institute of Technology (RIT), the Rochester Police Department (RPD), and criminology partners from the University at Albany. Existing OpenBWC components focus on audio and text workflows—transcription, speaker diarization, and human-in-the-loop correction—producing time-aligned transcripts for downstream analysis. These capabilities support queries over *what was said* and *when it was said* [1].

However, the transcripts are just the spoken language, and as such, cannot account for the shared situational context or the physical dynamics of an encounter. For example during

<sup>1</sup>OpenBWC is an on-site, access-controlled multi-sensory system co-designed with Rochester Police Department (RPD) partners to assist in the privacy-governed research and reviewing of BWC incidents. <https://openbwc.org/>

a typical interaction the officer and the other person treat the premises and the ongoing actions as common ground, resulting in speakers not frequently articulating the particulars. Consequently, the video record supplies critical review-relevant information that is not generally included in the transcript, such as the officer being in a patrol vehicle, on a street, approaching a doorway or in a house. The paper introduces a visual understanding layer and provides additional contextual and activity information in the form of time-stamped labels, which leads to the following research questions:

**RQ1.** Do 10-second video windows mostly show stable parts of an encounter?

**RQ2.** How much of the footage is difficult to label due to darkness and does that problem happen mostly in specific incidents?

**RQ3.** Do the patterns of physical activity look different depending on the operational context?

**RQ4.** Using minimal baseline models, can we predict the operational context more reliably than the level of motion intensity?

**RQ5.** When the model gives a low-confidence prediction, does that tend to align with the windows that human annotators also found difficult?

For RQ1–RQ3 we perform dataset audits (Section III-C). We answer RQ4 and RQ5 with predictive evaluation and error analysis (Section V).

In summary we make the following contributions:

- **a reproducible visual timeline method** that keeps privacy intact (no face/person recognition) and gives a clear, time-stamped, auditable index.
- **a labeling scheme** that is based on what can be seen in real BWC footage conditions.
- **simple, transparent baseline classification models** that require minimal supervised training.
- **an evaluation approach** combining class-wise metrics and confusion matrices.

This paper is structured as follows. Section II reviews related work in BWC research. Section III describes the data corpus, windowing process and annotation protocol. Section IV presents the modeling approach. Section V shows the experimental setup. Section VI concerns limitations. Section VII concludes and Section VIII lists future directions.

## II. RELATED WORK

Prior work on police BWC footage comes from fields such as criminology, public policy and computer science. For this paper, we focus on the following related areas: outcomes, structured coding, review systems, and egocentric video understanding.

Early research on police BWCs looked into why departments decided to start using them, what kinds of problems arose during the process and the bigger debates about making policing more open and holding officers accountable [2]. Studies moved toward trying to measure actual effects, such as whether activated cameras led to fewer instances where

officers used force, or fewer complaints against the police [3].

BWCs became material that could be coded, compared and studied across incidents. In that setting, video-based systematic social observation [4], [5] and related coding approaches showed that encounters could be analyzed in a consistent way across many cases [6]. Holladay and Makin offer one example through their work on incivility in one-on-one encounters drawn from archival BWC footage [7]. Their study shows that structured behavioral coding is useful and that it still needs a lot of human judgment. A related work has grown around transcripts generated from BWC audio. So researchers have used these transcripts to check officer communication mostly during traffic stops [8] and to apply natural language processing methods to support officer training and review of police-citizen interactions [9].

Watching manually hours of BWC footage can be time-consuming. Annotation tools were created out of necessity to transform unstructured video into usable datasets for testing and training as well as future modeling. More recent developments have included the release of web-based platforms specifically created for labeling police BWC footage. CVAT-BWV is an open-source extension of the Computer Vision Annotation Tool (CVAT) [10]. CVAT-BWV is built to be deployed locally to ensure that departments can host the program on their own computers rather than uploading media to a third party cloud. The platform includes features such as automatic speech recognition to automatically generate transcripts, speaker diarization, object detection and face related functionalities that support privacy. These tools allow departments to reduce time input for labeling videos, ensure better consistency between labels and allow for more annotators. Work with real-world BWC benchmark datasets shows that generalization remains a major challenge for machine learning models. Results often weaken when models are tested on footage from a different department, a new camera model or another mounting angle [11].

Existing research into computer vision, described this as a “high-impact, but technically challenging space,” which focused on the discrepancy between what the agency needs and what the unedited video from BWCs can provide [12]. More recent research focused on the development of learning-based approaches to BWC video recognition. For example semi-supervised first-person activity recognition explores how to exploit unlabeled BWC data to reduce annotation demand and stabilize learning when labeled examples are scarce [13]. A complementary work takes the problem less in terms of “which action is occurring” and more in terms of “the degree of movement exhibited by the camera wearer.” Research into ego-motion classification suggests that the dynamics of the motion can carry a significant portion of the information that is useful such as walking, running, and fast acceleration even when the visual information is degraded [14]. Researchers have long made use of representations of motion, such as optical flow, to segment or characterize the different phases of the video, as they summarize the information over the course of the video [15].

The recent advances in video models and vision-language pretrained models may also open the door for alternative solutions for video-based retrieval and labeling that do not rely on task-specific models [16], [17], [18]. In particular, the interest in vision-language models such as CLIP<sup>2</sup> has revived interest in zero-shot classification schemes [19], [20]. Nevertheless, in order to utilize these models in the context of BWC, there are also additional factors including data-use policies for agencies, redactions that may obscure the information at the level of persons, and the need to simplify model outputs existing schemas, rather than semantic knowledge graphs.

### III. DATA

This section documents the video corpus and data artifacts used for this research, as well as the deterministic windowing, annotation taxonomy and audits used to verify integrity and characterize uncertainty.

#### A. Video Corpus

This work employs a subset of RPD BWC videos maintained and processed by the OpenBWC project team through RIT Research Computing (RC) [21]<sup>3</sup>. This subset includes various BWC video camera types, which provide a variety of field-of-view perspectives, lens types, image stabilization modes and video recording settings. Lighting conditions also show considerable diversity across the videos. Due to the evidentiary nature of the videos, the MP4 videos are kept unchanged. We provide a reference to the original incident video and the interval at which the incident happened. By “curated,” we mean that we selected a smaller subset from the full set while still preserving a range of recording conditions.

Before windowing, annotating or training models we automatically performed a readiness assessment for each video. This process for a video includes: (i) opening the file and parsing stream metadata, (ii) decoding the first frame, excluding metadata parsing failures and (iii) extracting basic information from the video file. Table I shows the readiness results and dataset statistics for the subset used in this study.

TABLE I  
SCOPE OF THE CURATED RPD BWC CORPUS USED IN THIS STUDY.

Measure	Value
Incident videos	15
Total footage (hr)	2.19
Video duration (sec)	min 233.43, max 1131.93
Frame rate (fps)	min 29.97, max 30.00
Total windows	783

Using the MP4 videos that we validated, we divide each incident video  $v$  into non-overlapping windows of fixed length  $L = 10$  seconds. This gives  $N_v = \lfloor D/L \rfloor$  complete windows, where  $D$  denotes the video duration. Each window is mapped

to a timestamp interval  $[t, t + L)$ . We discard the remaining portion of the video, if any, so that every labeled window has the same 10-second length.

#### B. Annotation Taxonomy

We assign two labels to each 10-second video window: a context label, which describes the type of scene, and an activity label, which describes the intensity of motion, as shown in Tables II and III. The labels are descriptive and only use information visible within the window. Labels do not include any information about the identities of persons seen in the video, or make judgments about behavior or performance. When visual evidence is limited, annotators use low-evidence labels. These labels are a core design choice of this work because they avoid forced guessing, reduce noisy supervision, and prevent overconfident labeling.

TABLE II  
DEFINITIONS OF THE OPERATIONAL CONTEXT LABELS.

Label	Definition
PATROL_VEHICLE	Distinct vehicle interior structure (dashboard, windshield framing, steering wheel), frequent reflections and vehicle-interior viewpoint cues typical of driving.
OUTDOOR	Open environment signals such as streets, sidewalks, sky, building exteriors, parked vehicles and large depth range.
INDOOR	Clear interior signals such as walls, ceilings, door-frames, hallways, indoor lighting and enclosed surfaces.
LOW_VIS	Insufficient visual evidence due to darkness, blur, occlusion (hand/clothing), and camera-down. This label represents uncertainty.

TABLE III  
DEFINITIONS OF THE ACTIVITY LABELS.

Label	Definition
ROUTINE	Controlled motion, low-to-moderate motion magnitude and stable window-level behavior.
FOOT_PURSUIT	Sustained fast forward motion, large motion magnitudes with consistent direction across the window.
HIGH_ACTIVITY	Irregular high motion and magnitude with low directional coherence and high variance.
UNKNOWN	Window lacks reliable visual evidence to assess motion level.

Because of the labor-intensive nature of manual labeling, we only sample a subset of the window inventory for labeling purposes. Let us denote the set of all 10-second windows generated from the corpus as  $\mathcal{W}$ , and let us denote the subset of these windows that are labeled as  $\mathcal{W}_L \subset \mathcal{W}$ , where  $|\mathcal{W}_L| = 428$ . Sampling is done separately for each video. From the ordered set of windows based on `start_time`, we select  $k_{\text{cov}}$  windows (number of windows that should span the entire incident timeline) that are approximately evenly spaced, then select  $k_{\text{rand}}$  windows uniformly at random from the remaining windows using a constant seed for reproducibility. The video quota for sampling is  $k_{\text{cov}} + k_{\text{rand}}$  (fixed within a run), up to the total number of windows available in the video.

<sup>2</sup>CLIP = Contrastive Language-Image Pretraining

<sup>3</sup>RIT RC is the university’s centrally managed research computing environment that provides high-performance computing and research data storage services under institutional access controls.

**Dominant-time rule.** In cases where there are multiple labels, the label that appears the most in the given window of 10 seconds is assigned. To differentiate between cases of clear supervision and boundary cases, the `context_transition` and `activity_transition` flags are also recorded. These flags are assigned the value of 1 if a change in context and/or activity transpires in the window of 10 seconds.

### C. Dataset auditing

Before any modeling, a series of automated dataset audits are performed to check the structural correctness of the dataset and understand the uncertainty and temporal behaviors within the annotated window.

**Dataset quality checks.** We verified that the dataset had the following properties: that it contains 428 unique window keys, and has zero missing labels and out-of-vocabulary values. In addition, we ensured that all window keys point to valid entries.

**Label distributions.** We summarize the label distributions to show class imbalance and the share of low-evidence windows. The results in Table IV show that OUTDOOR is the context we see often, making up 48.36% of the time, and ROUTINE is the activity that happens most, which is 80.84%. When it comes to uncertainty, 19.16% of labeled windows are classified as LOW\_VIS. This means about one out of every five windows does not give us information to figure out the context. On the other hand, we do not see UNKNOWN activity very often only 1.17% of the time. This suggests that we can usually tell how intense the motion is, even if the window is not ideal. In our sample every time we saw UNKNOWN activity it was due to context. Still, we do not treat this as a general rule. In a larger and more varied dataset, other conditions such as glare, overexposure, strong motion blur or upward camera angles could also make activity difficult to label.

TABLE IV  
CLASS DISTRIBUTION IN THE LABELED SUBSET.

Context	Count	%
OUTDOOR	207	48.36
LOW_VIS	82	19.16
PATROL_VEHICLE	71	16.59
INDOOR	68	15.89
Activity	Count	%
ROUTINE	346	80.84
HIGH_ACTIVITY	53	12.38
FOOT_PURSUIT	24	5.61
UNKNOWN	5	1.17

**Context–activity relationship.** We next test whether context and activity labels are statistically independent. Table V reports conditional rates suggesting a small-to-moderate dependence between context and activity.

TABLE V  
CONDITIONAL ACTIVITY DISTRIBUTION GIVEN CONTEXT LABELS.

	ROUTINE	HIGH_ACTIVITY	FOOT_PURSUIT	UNKNOWN
INDOOR	0.868	0.088	0.044	0.000
OUTDOOR	0.816	0.082	0.101	0.000
PATROL_VEHICLE	0.958	0.042	0.000	0.000
LOW_VIS	0.610	0.329	0.000	0.061

In OUTDOOR windows FOOT\_PURSUIT occurs 10.1% of the time. PATROL\_VEHICLE windows are predominantly ROUTINE. UNKNOWN activity occurs only when context is LOW\_VIS and within LOW\_VIS windows, UNKNOWN happens 6.1% of the time.

**Temporal stability.** In Table VI we examine how frequently the labels change between adjacent labeled windows. The overall context change rate is  $\bar{r}(\text{context}) = 0.1356$ , while the activity change rate is  $\bar{r}(\text{activity}) = 0.1719$ . This indicates that shifts in activity tend to occur somewhat more often than changes in scene.

TABLE VI  
MOST FREQUENT LABEL TRANSITIONS BETWEEN ADJACENT WINDOWS.

Context	Count	Activity	Count
OUT→OUT	178	R→R	306
LV→LV	62	H→R	20
OUT→LV	13	R→H	17

*Abbrev:* OUT=OUTDOOR, PV=PATROL\_VEHICLE, IN=INDOOR, LV=LOW\_VIS; R=ROUTINE, H=HIGH\_ACTIVITY, F=FOOT\_PURSUIT.

Figure 1 provides a more detailed view of adjacent-window transition patterns for both label spaces.

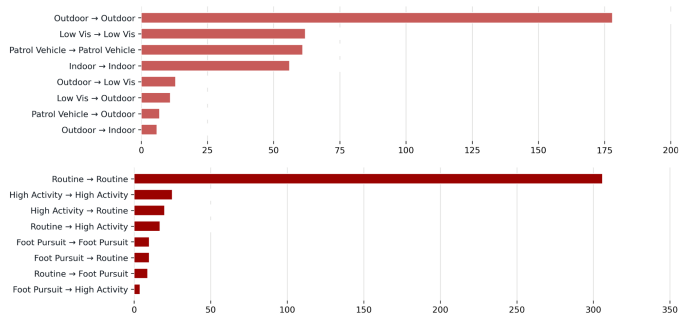


Fig. 1. Most frequent transitions between adjacent labeled windows in the labeled subset. Top: context transitions. Bottom: activity transitions.

In the context labels, self-transitions are by far the most common. When the label does change, it is usually between just a handful of pairs, especially OUTDOOR flipping back and forth with LOW\_VIS. Overall, it shows that the scene labels tend to stay stable from one window to the next. The activity labels follow a similar pattern, with self-transitions dominating. ROUTINE→ROUTINE is more frequent than anything else. That said, activity labels switch between neighboring windows more often than

context does, particularly bouncing between ROUTINE and HIGH\_ACTIVITY.

**Run-length behavior.** In addition to considering the rate at which the label of adjacent windows differs, it is also useful to consider how long any individual label remains visible. This provides a distinct axis along which to judge the temporal structure of the context and activity. There is clearly some persistence in the context. For PATROL\_VEHICLE the median run length was 4 windows, with a mean of 7.35 windows. For the three settings OUTDOOR, INDOOR and LOW\_VIS, the median run lengths were 3 windows each, with mean run lengths of 4.15, 4.69 and 4.71 windows, respectively. The persistence of an activity state is measured in terms of both the median length of the longest contiguous run of windows and the mean run length. For the most common activity state, the majority of the longest runs of contiguous windows that were analyzed consisted entirely of ROUTINE and had a length of 5 windows. The mean run length for ROUTINE was 8.65 windows. In contrast, the briefly mentioned FOOT\_PURSUIT, HIGH\_ACTIVITY and UNKNOWN each had a median run length of 1 window and, accordingly, a mean run length of 1.71, 1.89 and 1.25 windows, respectively.

**Within-window transition burden.** We also looked at how often there was a shift inside a single 10-second window. In the labeled data, 61 out of 428 windows (about 14.3%) had at least one internal transition. Most of them were activity-only shifts (36 windows or 59%) and the next most common were context-only shifts (17 windows or 27.9%). Just 8 windows (13.1%) had activity and context changes at the same time. These boundary problems usually happen because of changes in how much someone is moving, not because the scene itself changes suddenly. It also makes it clear why we should keep those explicit transition flags, so we can take those difficult windows out and look at them separately when we look at or review the results.

**Annotator agreement.** To estimate labeling consistency, we compare two full labeling passes done by human annotators over the same labeled window set  $\mathcal{W}_L$ . We report exact-match agreement and Cohen’s  $\kappa$

$$\text{Acc}(y) = \frac{1}{|\mathcal{W}_L|} \sum_{w \in \mathcal{W}_L} \mathbb{I}[y^{(1)}(w) = y^{(2)}(w)] \text{ and}$$

$$\kappa = \frac{p_o - p_e}{1 - p_e},$$

where  $p_o$  is the observed agreement and  $p_e$  is the chance of agreement, which we compute from the marginal label distributions.

As shown in Figure 2, the context labels are more consistent across passes than the activity labels. Activity agreement remains fairly strong, but it shows more variation across passes. Most of that movement comes from windows where

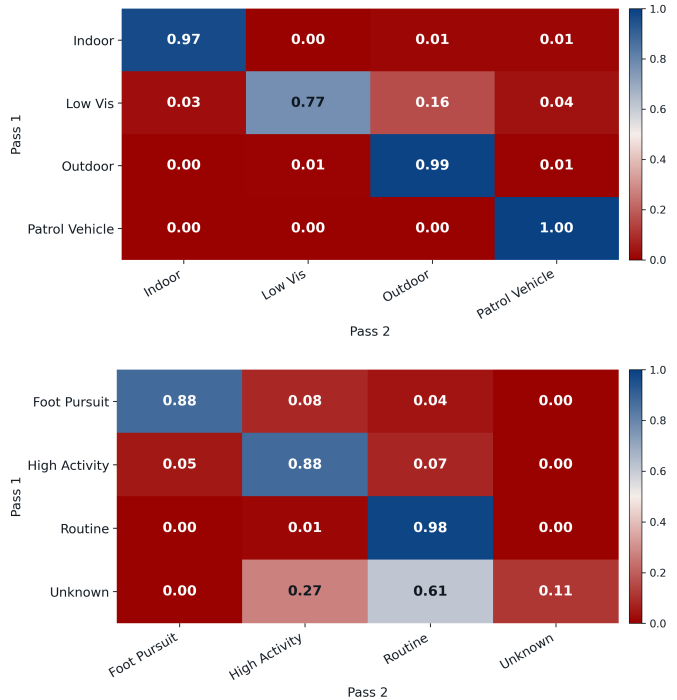


Fig. 2. Row-normalized agreement matrices comparing human annotator labels from Pass 1 and Pass 2. Top: context agreement. Bottom: activity agreement.

the visual evidence is limited. In the context label space, agreement is strongly concentrated on the diagonal, especially for PATROL\_VEHICLE, OUTDOOR and INDOOR, while most disagreement involves LOW\_VIS, which is occasionally reassigned to neighboring scene categories. In the activity label space ROUTINE is the category that annotators agree on the most. Both FOOT\_PURSUIT and HIGH\_ACTIVITY show moderate agreement. The main source of disagreement is UNKNOWN. When labels are marked as UNKNOWN in Pass 1, they are often changed in Pass 2, most commonly to ROUTINE or HIGH\_ACTIVITY.

These results confirm the fixed-window representation employed in this study. The timelines show significant temporal stability (RQ1). Uncertainty is constrained on challenging instances (RQ2). The observed connection between context and activity also shows that the representation captures important structure in police encounters (RQ3).

## IV. METHODS

### A. Platform Description

**GroundTruth** is a web-based application that helps to label BWC videos for the OpenBWC timeline. GroundTruth is hosted in a secure environment. Saved labels are exportable for later review, training and evaluation. GroundTruth distinguishes itself from other labeling tools, since quick decisions on small parts of a video at a time are made handling scenarios with limited evidence where typically

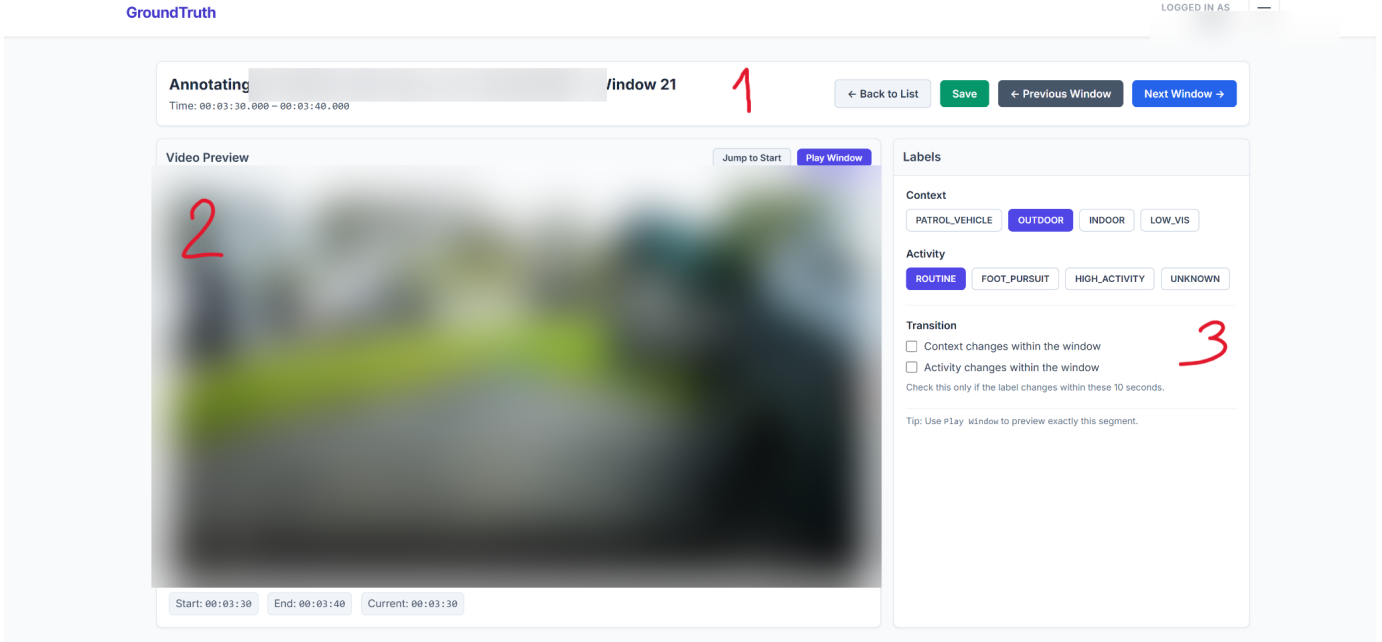


Fig. 3. GroundTruth window-level annotation interface (video preview is intentionally blurred in this paper for privacy reasons). For every 10-second window, a set of clipped timestamps is given requiring one context and one activity label from a fixed vocabulary. Annotators can optionally mark transitions happening within one window.

some boundary ambiguity exists, without allowing users to make wrong guesses.

**User interface.** There are three main parts of the main annotation screen (see Figure 3).

- 1) Window header: This area displays information about the segment to be annotated such as the incident ID, the specific window within the video that this segment is drawn from and the start and end timestamps of the annotated segment.
- 2) Video panel: A preview player which displays a portion of the video the user is currently annotating. The user can navigate to the beginning of the currently selected segment and can play the same segment back again.
- 3) Label panel: The annotator must select one context label and one activity label from a fixed vocabulary, and additionally can select a flag indicating whether or not there is any change within that segment.

## B. Visual Timeline Pipeline

In this work, we frame the task of visual timeline construction into two window-level supervised classification tasks. Namely, (i) operational context classification and (ii) activity (motion intensity) classification.

Figure 4 shows the four stages of the workflow. In **(1) Data Preparation**, BWC videos are partitioned into timestamped windows. In **(2) Human Knowledge**, some of these windows are labeled by a human annotator using the controlled label space. In **(3) Prediction**, time windows are analyzed. From

a features perspective, lightweight classifiers are trained in a supervised fashion only using the labeled subset of time windows. The resulting models can then be used to predict the labels and the corresponding confidence scores for all windows in the video. In **(4) Operational Use**, the predicted streams are used to generate unified timeline that can be consumed by OpenBWC or more general law enforcement applications. The dashed line in the evaluation loop indicates that the evaluation results can be used to adjust the thresholds and the sampling policies without modifying the window representation. A pseudocode description of the full timeline generation procedure is provided in Appendix A.

## C. Operational Context Inference

### a) CLIP embeddings.

For each window  $w_i$ , we sample  $K$  frames (endpoint excluded) and decode the corresponding keyframes  $\{I_{i,1}, \dots, I_{i,K}\}$ . We use a pretrained OpenCLIP image encoder<sup>4</sup> as a fixed feature extractor. Let  $\Phi(\cdot)$  denote the frozen image encoder with the pretrained weights specified by our extraction configuration, i.e., the (model\_name, pretrained) pair. For each sampled keyframe  $I_{i,k}$  in window  $w_i$ , we compute an image embedding

$$\mathbf{z}_{i,k} = \Phi(I_{i,k}) \in \mathbb{R}^d, \quad (1)$$

<sup>4</sup>OpenCLIP is an open-source implementation and set of pretrained CLIP models trained on large-scale image-text pairs: [https://github.com/mlfoundations/open\\_clip](https://github.com/mlfoundations/open_clip)

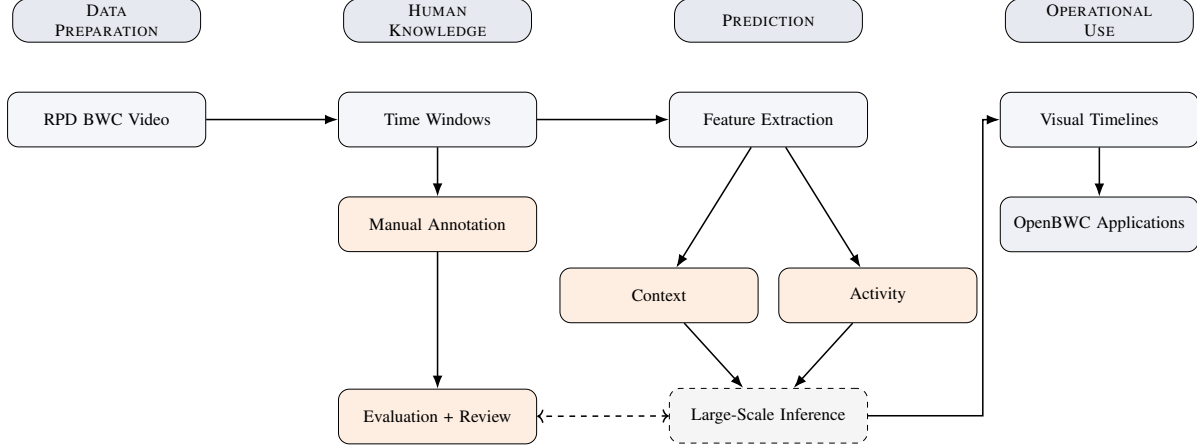


Fig. 4. End-to-End Visual Analysis Pipeline.

and apply  $\ell_2$  normalization

$$\tilde{\mathbf{z}}_{i,k} = \frac{\mathbf{z}_{i,k}}{\|\mathbf{z}_{i,k}\|_2}. \quad (2)$$

This normalization has the effect of removing dependence on the magnitude of the embeddings and greatly increasing the stability of the pooled descriptor,  $\Pi \in \{\text{MEAN}, \text{MAX}\}$ , across sampled frames. To get a single descriptor per window, the normalized keyframe embeddings are then aggregated in a deterministic manner

$$\mathbf{z}_i = \Pi(\{\tilde{\mathbf{z}}_{i,1}, \dots, \tilde{\mathbf{z}}_{i,K}\}). \quad (3)$$

The resulting window descriptors are then stacked up to form a feature matrix  $\mathbf{Z} \in \mathbb{R}^{N \times d}$ .

#### b) Context classifier.

We perform a supervised training on a multiclass logistic regression classifier. This is done using the pooled OpenCLIP window embeddings,  $\mathbf{z}_i$ . To reduce leakage from temporally adjacent windows within the same incident, we split at the video level. Let  $\mathcal{Z}_{\text{Context}}$  denote the operational context label set defined in Table II. Given a window embedding,  $\mathbf{z}_i$ , the classifier outputs class probabilities,  $\mathbf{p}_i = h_\theta(\mathbf{z}_i)$  giving the predicted probability for each context class  $c \in \mathcal{Z}_{\text{Context}}$

$$s_{\text{ctx},i} = \max_c \mathbf{p}_i(c).$$

If a confidence threshold is enabled, any predictions where  $s_{\text{ctx},i} < \tau_{\text{ctx}}$  are labeled as LOW\_VIS.

#### D. Activity Inference

##### a) Feature representations.

As an appearance baseline for activity, we compute a per-window representation using the same OpenCLIP encoder and pooling procedure described in IV-C0a. For activity, we evaluate two modes: (1) clip, which uses only the pooled embedding and (2) clip\_delta, which appends three temporal-stability scalars computed from the frame embeddings: the mean and maximum cosine distance between

consecutive frame embeddings and the mean per-dimension embedding standard deviation across frames.

As a motion-based representation, we compute dense optical flow using Farneback’s method between consecutive grayscale frames, producing up to  $K - 1$  flow fields [22]. We summarize motion over the window with a compact, interpretable feature vector

$$\mathbf{x}_i = \Psi(\{\mathbf{u}_{i,k}\}_{k=1}^{K-1}) \in \mathbb{R}^m. \quad (4)$$

Specifically, for each video, we use the means and standard deviations of the magnitude of flow, magnitude of the direction of flow, magnitude of the global mean flow, simple frame quality measures, and the number of successfully decoded frames  $n_{\text{frames}}$  out of  $K$  samples from a video. For each video, we then assign  $n_{\text{frames}}$  as the number of successfully decoded frames. If less than two frames were decoded, we set the flow-based quantities to zero while retaining  $n_{\text{frames}}$ . The computed summaries include 12 dimensional feature vectors.

We also examine whether appearance cues help improve activity when combined with motion information. Given  $\mathbf{x}_i^{(\text{clip})} \in \mathbb{R}^{d_c}$  and  $\mathbf{x}_i^{(\text{flow})} \in \mathbb{R}^{d_f}$ , we perform per-block  $z$ -scoring on the dataset,  $b \in \{\text{CLIP}, \text{FLOW}\}$ ,

$$\tilde{\mathbf{x}}_i^{(b)} = \frac{\mathbf{x}_i^{(b)} - \mu_b}{\sigma_b},$$

where  $\mu_b$  and  $\sigma_b$  are the per-dimension mean and standard deviation of block  $b$ . The final concatenated feature is then

$$\mathbf{x}_i^{(\text{fused})} = [\tilde{\mathbf{x}}_i^{(\text{clip})}; \tilde{\mathbf{x}}_i^{(\text{flow})}] \in \mathbb{R}^{d_c+d_f}. \quad (5)$$

##### b) Activity classifier.

The model is trained to predict over the activity label set  $\mathcal{Z}_{\text{Activity}}$  defined in Table III and is implemented as a multiclass classifier  $g_\phi$ , trained on window feature vectors  $\mathbf{x}_i$ . For a window feature vector  $\mathbf{x}_i$ ,  $g_\phi$  emits a distribution over class probabilities  $\mathbf{q}_i = g_\phi(\mathbf{x}_i)$ , where  $\mathbf{q}_i(a)$  denotes the predicted

probability of activity class  $a \in \mathcal{Y}_{\text{Activity}}$ . The predicted label with its confidence score is calculated as

$$s_{\text{act},i} = \max_a \mathbf{q}_i(a).$$

For uncertain evidence, we support filtering based on a “confidence” score. If the score for a given result  $s_{\text{act},i} < \tau_{\text{act}}$ , it is classified as UNKNOWN.

## V. EVALUATION

### A. Experimental setup

We approach the context and activity recognition tasks as supervised window-level classification tasks, by partitioning each video into non-overlapping windows and performing hold-out splits on the video-level. We report the performance on the clean test windows (non-transition regions), and note that transition-flagged windows can potentially have multiple labels, making single-label performance ambiguous.

**Compared runs.** We present an in-depth study on key aspects of our method. For contextualization, we present a small set of “easy” ablations around the frozen visual backbone of the OpenCLIP model, the number of frames we sample within each window, and the pooling method. For activity, we also explore three different representation families: (i) using the motion information provided by optical-flow, (ii) using the embeddings from CLIP with varying frames and pooling and (iii) a fused version of (i) and (ii) where we concatenate the CLIP-derived features with the optical-flow features. In Table VII we provide a complete map of our experiments and how we have split the runs for computing the statistics.

### B. Results

#### a) Context.

The results of the window-level context performance are shown in Table VIII, which is based on the held-out clean test split. We can see that the performance is consistent across the four different runs, with accuracy ranging from 75.00% to 78.75%, and macro-F1 ranging from 0.7300 to 0.7500.

TABLE VIII  
CONTEXT RESULTS ON HELD-OUT TEST WINDOWS.

Run	Accuracy	Macro-F1
E1	78.75%	0.7500
E2	78.75%	0.7300
E3	75.00%	0.7300
E4	77.50%	0.7500

Overall, these results suggest that the context task is quite robust to moderate changes in frame sampling and pooling when the CLIP features are frozen. However, using a larger backbone, such as ViT-L/14, does not seem to provide any benefits in this setting, as E3 has the lowest accuracy and does not improve macro-F1. Similarly, increasing the number of sampled frames from 5 to 10 under mean pooling does not

improve performance, as E2 has the same accuracy as E1 but lower macro-F1. On the other hand, max pooling at  $K = 10$ , as used in E4, slightly improves class balance and achieves the best macro-F1 score, tied with E1.

Here we take a closer look at the confusion matrices, displayed in Figures 5 and 6.

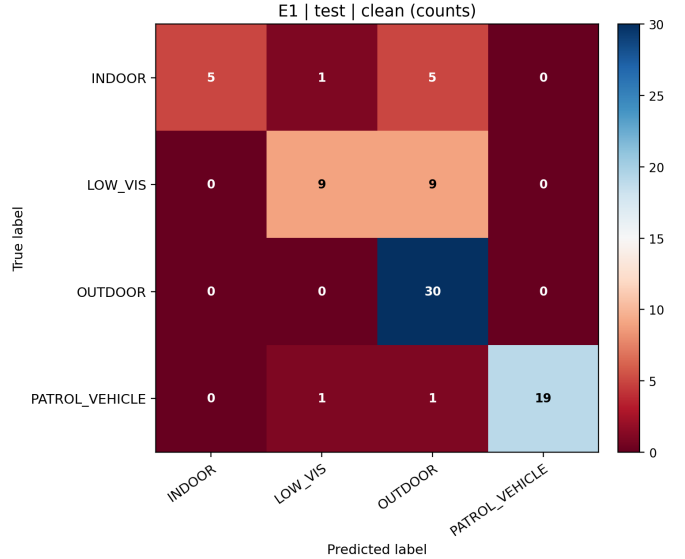


Fig. 5. Operational context confusion matrix on the held-out clean test split for E1.

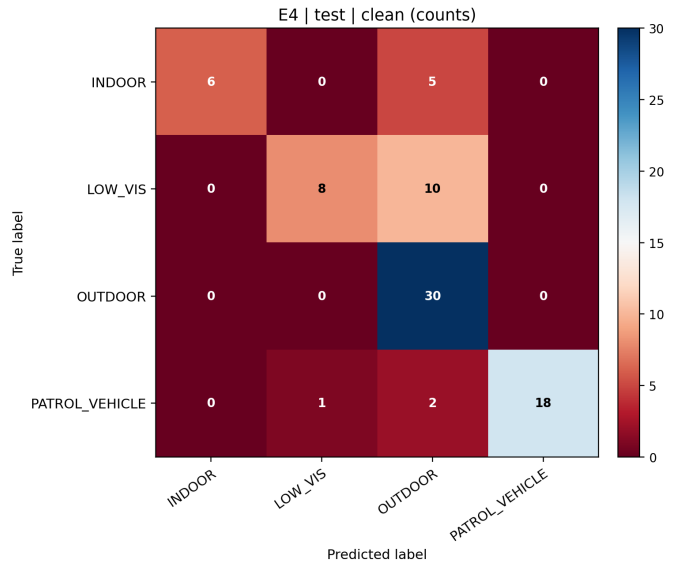


Fig. 6. Operational context confusion matrix on the held-out clean test split for E4.

Looking across runs, we see that context errors are not randomly distributed across all the classes. Rather, there are some that are recognized very consistently, such as OUTDOOR, while others such as PATROL\_VEHICLE are

TABLE VII  
EXPERIMENT MAP FOR EVALUATION RUNS, GROUPED BY TASK AND REPRESENTATION FAMILY.

Task	Run	Model setting	Run	Model setting
Context (CLIP)	E1	ViT-B/32; $K=5$ ; mean	E2	ViT-B/32; $K=10$ ; mean
Context (CLIP)	E3	ViT-L/14; $K=5$ ; mean	E4	ViT-B/32; $K=10$ ; max
Activity (Flow)	F1*	$K=5$ ; $224 \times 126$ ; w15; L3; it3	F2*	$K=10$ ; $320 \times 180$ ; w15; L3; it3
Activity (Flow)	F3*	$K=10$ ; $320 \times 180$ ; w9; L3; it3	F4*	$K=10$ ; $320 \times 180$ ; w21; L3; it3
Activity (Flow)	F5*	$K=10$ ; $320 \times 180$ ; w21; L4; it3	F6*	$K=10$ ; $320 \times 180$ ; w21; L3; it5
Activity (CLIP)	A1*	ViT-B/32; $K=10$ ; mean	A2*	ViT-B/32; $K=10$ ; max
Activity (CLIP + $\Delta$ )	A3*	ViT-B/32; $K=10$ ; mean	A4*	ViT-B/32; $K=10$ ; max
Activity (CLIP + $\Delta$ )	A5*	ViT-B/32; $K=5$ ; mean	A6*	ViT-B/32; $K=20$ ; mean

$W \times H$  denotes resize resolution;  $w$  is Farnebäck window size;  $L$  is the number of pyramid levels;  $it$  is the number of iterations per level.

\* Activity feature configurations eligible for fusion (AF). Only the fused combinations reported in the results section were evaluated.

recognized relatively consistently, and are usually correctly discriminated from the other contexts. Most errors fall in the boundary cases between INDOOR, LOW\_VIS and OUTDOOR. These errors are not class collapse (i.e., all misclassified as the same class). Rather, they are instances where it is difficult to tell whether a given excerpt of video is one of these three contexts. Therefore, the main challenge in this task is not class collapse, but rather, distinguishing contexts that are very close visually in BWC settings.

To help us understand these patterns better, we show the most common recurring confusions across all runs in Appendix B. Figure 8 shows that most of the mistakes happen in a small number of transition types instead of being spread out evenly. LOW\_VIS  $\rightarrow$  OUTDOOR is the most common mistake in all of the experiments. Confusions involving LOW\_VIS as a target class, on the other hand, are still rare and stable. In general this shows that the main cause of error is not random misclassification, but systematic confusion between contexts that look similar.

#### b) Activity.

The detailed activity evaluation reveals a substantially more challenging task than is reflected in the clean-summary metrics. While overall accuracy ranged from 82.50% to 88.33% and macro-F1 from 0.3491 to 0.4535, performance was largely dominated by the majority class ROUTINE achieving high F1. The rarely occurring class FOOT\_PURSUIT was not detected by any run. The main differences between the individual runs are in their F1 on the class HIGH\_ACTIVITY, which is the second most frequent class after ROUTINE. The ablations primarily affect performance on the moderately rare dynamic activity class HIGH\_ACTIVITY.

Macro-F1 is a better evaluation metric than accuracy for this task. The best non-fused run is A6, and the best overall run is AF6. The fused representations improve the balanced performance over the corresponding CLIP-based models, indicating that appearance and motion are complementary for activity prediction (see Table IX).

We show the strongest non-fused activity model in Figure 7 on the held-out test set. While the ROUTINE class is recognized very well in both cases, the fused model im-

TABLE IX  
ACTIVITY RESULTS ON THE HELD-OUT TEST WINDOWS.

Run	Representation	Accuracy	Macro-F1
A1	CLIP	85.00%	0.3740
A2	CLIP	85.83%	0.3785
A3	CLIP + $\Delta$	82.50%	0.3491
A4	CLIP + $\Delta$	85.00%	0.3883
A5	CLIP + $\Delta$	85.00%	0.3981
A6	CLIP + $\Delta$	88.33%	0.4243
AF1	Fused	86.67%	0.4512
AF2	Fused	86.67%	0.4058
AF3	Fused	83.33%	0.3696
AF4	Fused	85.00%	0.3883
AF5	Fused	85.00%	0.4334
AF6	Fused	87.50%	0.4535

proves balanced performance most in terms of recognizing more HIGH\_ACTIVITY instances, while FOOT\_PURSUIT remains to be a challenging class in all activity runs.

Figure 9 in Appendix B shows the common recurring activity confusions across the CLIP-based runs. The common mistake is UNKNOWN turning into HIGH\_ACTIVITY. This mistake shows up in all models. On the other hand, UNKNOWN turning into ROUTINE does not happen very often. This mistake stays the same every time we run the system. So when the input is not clear the system is more likely to think there is movement than no activity. This shows how difficult it is to tell the difference between weak signals and real dynamic behavior using only appearance features.

The fused models in Figure 10 in Appendix B show a similar pattern. Fusion makes the class balance better overall, but the most common confusion is still UNKNOWN  $\rightarrow$  HIGH\_ACTIVITY, with a few more counts in some runs. The fact that UNKNOWN  $\rightarrow$  ROUTINE is the same across all runs shows that the main problem is figuring out how to deal with unclear visual evidence, not how to separate clearly defined activity states.

RQ4 asked if simple baseline models are better at predicting operational context than motion intensity. The findings indicate that the response is affirmative. Even though activity accuracy was sometimes high, this was mostly because of the

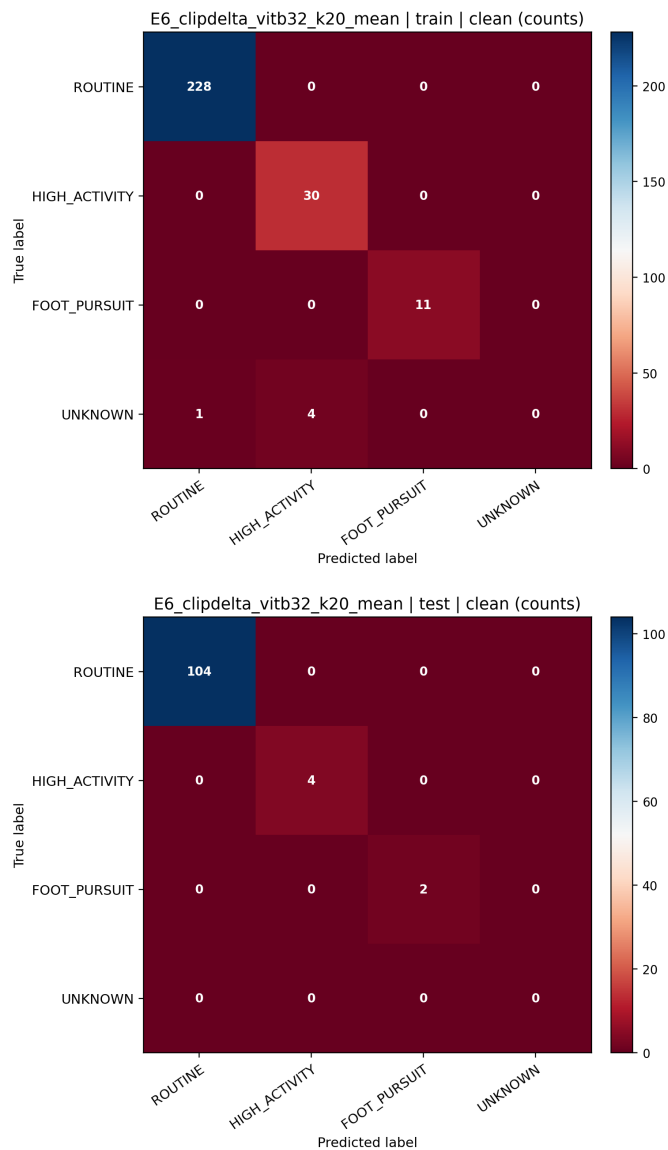


Fig. 7. Activity confusion matrices for the strongest non-fused run (A6) run. Top: train set. Bottom: test set.

dominant ROUTINE class.

**RQ5** asked if model predictions with low confidence tend to match windows that human annotators also found challenging. The findings indicate that this occurs frequently. For both tasks, uncertainty was mostly found in windows with weak or unclear evidence, such as darkness, occlusion and transition areas. The confidence-based flagging behavior seems to show not only how uncertain the model is, but also how difficult it is for people to label windows.

## VI. DISCUSSION

The proposed visual timelines suggest that a fixed window approach can provide a useful overview of setting and activity level while remaining consistent with the privacy requirements

of the data. The variability seen across the incidents also suggests that a 10-second window is a useful window size for indexing, model development and review. The approach has several *limitations*:

Using fixed-size with non-overlapping windows can cause short transitions near the window boundaries to be “smoothed over.”

The activity labels use relatively basic optical flow summary features. Although easy to understand the features provide limited descriptive information and may group visually different behaviors under the same label.

The size of the labeled set is still limited which determines the complexity of the model.

## VII. CONCLUSION

This work presented a reproducible method for organizing police BWC footage into visual timelines. The approach focuses on human annotation, dataset auditing and baseline models. The results showed that operational context was easier to recover (with  $F1=0.7500$ ) than motion intensity especially when behavior was unclear (with  $F1=0.4243$ ). The main contribution is a practical approach for supporting law enforcement review with structured visual information.

## VIII. FUTURE WORK

Next we will focus on linking transcript timestamps to the visual timeline so speech can be reviewed together with changes in scene and activity. We will also add a second review of uncertain windows that uses the surrounding parts of the same incident.

## ACKNOWLEDGMENT

This research is supported by Grant 15PBJA-22-GG-03328-BWCx with the U.S. Department of Justice through its Office of Justice Programs and Bureau of Justice Assistance, awarded to the City of Rochester.

## REFERENCES

- [1] A. Srbinovska, A. Srbinovska, V. Senthil, A. Martin, J. McCluskey, J. Bateman, and E. Fokoué, “Towards ai-driven policing: Interdisciplinary knowledge discovery from police body-worn camera footage,” 2025, arXiv. [Online]. Available: <https://arxiv.org/abs/2504.20007>
- [2] M. D. White, “Police officer body-worn cameras: Assessing the evidence,” Office of Community Oriented Policing Services (COPS Office), U.S. Department of Justice, Washington, D.C., USA, Tech. Rep. NCJ 247941, 2014. [Online]. Available: <https://www.ojp.gov/library/publications/police-officer-body-worn-cameras-assessing-evidence>
- [3] B. Ariel, W. A. Farrar, and A. Sutherland, “The effect of police body-worn cameras on use of force and citizens’ complaints against the police: A randomized controlled trial,” *Journal of Quantitative Criminology*, vol. 31, pp. 509–535, 2015. [Online]. Available: <https://doi.org/10.1007/s10940-014-9236-3>
- [4] J. McCluskey, C. D. Uchida, Y. Feys, and S. E. Solomon, “Video-based sso and body-camera data,” in *Systematic Social Observation of the Police in the 21st Century*. Cham: Springer, 2023, pp. 47–74. [Online]. Available: [https://doi.org/10.1007/978-3-031-31482-7\\_4](https://doi.org/10.1007/978-3-031-31482-7_4)

- [5] W. Terrill and L. Zimmerman, "Police use of force escalation and de-escalation: The use of systematic social observation with video footage police use of force escalation and de-escalation: The use of systematic social observation with video footage," *Police Quarterly*, vol. 25, no. 2, pp. 155–177, 2022. [Online]. Available: <https://nij.ojp.gov/library/publications/police-use-force-escalation-and-de-escalation-use-systematic-social>
- [6] R. E. Worden, B. P. Holladay, S. J. McLean, H. Cochran, and D. L. Reynolds, "Systematic social observation of police-citizen encounters: Coding and measurement through body-worn cameras," *Justice Quarterly*, vol. 42, no. 7, pp. 1410–1443, 2025. [Online]. Available: <https://doi.org/10.1080/07418825.2025.2463406>
- [7] B. P. Holladay and D. A. Makin, "Baselining incivility in one-on-one police encounters from bwc archival footage: Exploratory study of race, gender and contact type effects," *Police Practice and Research*, vol. 22, no. 6, pp. 1618–1636, 2021. [Online]. Available: <https://doi.org/10.1080/15614263.2021.1914040>
- [8] N. P. Camp, R. Voigt, M. G. Hamedani, D. Jurafsky, and J. L. Eberhardt, "Leveraging body-worn camera footage to assess the effects of training on officer communication during traffic stops," *PNAS Nexus*, vol. 3, no. 9, 2024. [Online]. Available: <https://doi.org/10.1093/pnasnexus/pgae359>
- [9] N. P. Camp and R. Voigt, "Body camera footage as data: Using natural language processing to monitor policing at scale & in depth," *Behavioral Science & Policy*, vol. 10, no. 2, pp. 16–25, 2024. [Online]. Available: <https://doi.org/10.1177/23794607241308636>
- [10] P. Hejabi, A. K. Padte, P. Golazizian, R. Hebbbar, J. Trager, G. Chochlakis, A. Kommineni, E. Graeden, S. Narayanan, B. A. T. Graham, and M. Dehghani, "Cvat-bwv: A web-based video annotation platform for police body-worn video," in *Proceedings of the Thirty-Third International Joint Conference on Artificial Intelligence, IJCAI-24*, 2024, pp. 8674–8678. [Online]. Available: <https://doi.org/10.24963/ijcai.2024/1006>
- [11] H. Sameer, J.-L. Dugelay, M. Rizal Mohd Isa, and M. Adib Khairuddin, "Moving forward with bwc: The faleb dataset for multimodal image analysis," in *IEEE International Conference on Image Processing*, 2025, pp. 1552–1557. [Online]. Available: <https://doi.org/10.1109/ICIP55913.2025.11084403>
- [12] J. Corso, A. Alahi, K. Grauman, G. D. Hager, L.-P. Morency, H. Sawhney, and Y. Sheikh, "Video analysis for body-worn cameras in law enforcement," Computing Community Consortium, Washington, D.C., USA, Tech. Rep. White Paper 11, 2015. [Online]. Available: <https://cra.org/ccc/wp-content/uploads/sites/2/2015/01/CCCWhitepaperonBodyCamerasinLawEnforcement.pdf>
- [13] H. Chen, H. Li, A. Song, M. Haberland, O. Akar, A. Dhillon, T. Zhou, A. L. Bertozzi, and P. J. Brantingham, "Semi-supervised first-person activity recognition in body-worn video," 2019, arXiv. [Online]. Available: <https://arxiv.org/abs/1904.09062>
- [14] Z. Meng, J. Sánchez, J.-M. Morel, A. L. Bertozzi, and J. P. Brantingham, "Ego-motion classification for body-worn videos," in *Imaging, Vision and Learning Based on Optimization and PDEs*. Cham: Springer, 2018, pp. 221–239. [Online]. Available: [https://doi.org/10.1007/978-3-319-91274-5\\_10](https://doi.org/10.1007/978-3-319-91274-5_10)
- [15] Y. Poleg, C. Arora, and S. Peleg, "Temporal segmentation of egocentric videos," in *IEEE Conference on Computer Vision and Pattern Recognition*, 2014, pp. 2537–2544. [Online]. Available: <https://doi.org/10.1109/CVPR.2014.325>
- [16] N. Madan, A. Møgelmoose, R. Modi, Y. S. Rawat, and T. B. Moeslund, "Foundation models for video understanding: A survey," 2024, arXiv. [Online]. Available: <https://arxiv.org/abs/2405.03770>
- [17] Y. Wang, K. Li, X. Li, J. Yu, Y. He, C. Wang, G. Chen, B. Pei, Z. Yan, R. Zheng *et al.*, "Internvideo2: Scaling foundation models for multimodal video understanding," in *Computer Vision – ECCV 2024*. Cham: Springer Nature Switzerland, 2024, pp. 396–416. [Online]. Available: [https://link.springer.com/chapter/10.1007/978-3-031-73013-9\\_23](https://link.springer.com/chapter/10.1007/978-3-031-73013-9_23)
- [18] F. Romero, C. Winston, J. Hauswald, M. Zaharia, and C. Kozyrakis, "Zelda: Video analytics using vision-language models," 2023, arXiv. [Online]. Available: <https://arxiv.org/abs/2305.03785>
- [19] A. Radford, J. W. Kim, C. Hallacy, A. Ramesh, G. Goh, S. Agarwal, G. Sastry, A. Askell, P. Mishkin, J. Clark, G. Krueger, and I. Sutskever, "Learning transferable visual models from natural language supervision," 2021, arXiv. [Online]. Available: <https://arxiv.org/abs/2103.00020>
- [20] M. Cherti, R. Beaumont, R. Wightman, M. Wortsman, G. Ilharco, C. Gordon, C. Schuhmann, L. Schmidt, and J. Jitsev, "Reproducible scaling laws for contrastive language-image learning," in *2023 IEEE/CVF Conference on Computer Vision and Pattern Recognition (CVPR)*, 2023, pp. 2818–2829. [Online]. Available: <https://doi.org/10.1109/CVPR52729.2023.00276>
- [21] R. I. of Technology, "Research computing services," 2026. [Online]. Available: <https://www.rit.edu/researchcomputing/>
- [22] G. Farneäck, "Two-frame motion estimation based on polynomial expansion," in *Image Analysis*, vol. 2749. Berlin, Heidelberg: Springer, 2003, pp. 363–370. [Online]. Available: [https://doi.org/10.1007/3-540-45103-X\\_50](https://doi.org/10.1007/3-540-45103-X_50)

---

**Algorithm 1: Visual Timeline Generator**

---

**Input** : Incident videos  $\mathcal{V}$ ; window length  $L = 10$ ; frames per window  $K$ ; frozen visual encoder  $\Phi$ ; pooling operator  $\Pi$ ; trained context classifier  $f_{\text{ctx}}$ ; activity feature extractor  $\Psi$ ; trained activity classifier  $f_{\text{act}}$ ; confidence thresholds  $\tau_{\text{ctx}}, \tau_{\text{act}}$ .

**Output**: A mapping of incident videos to window-level timeline records:  $\{\mathcal{T}(v)\}_{v \in \mathcal{V}}$ .

```

foreach  $v \in \mathcal{V}$  do
   $\mathcal{W} \leftarrow \text{MakeWindows}(v, L)$ 
   $\mathcal{T}(v) \leftarrow []$ 
  foreach  $w \in \mathcal{W}$  do
     $F \leftarrow \text{SampleFrames}(w, K)$ 
    // Context pathway
     $E \leftarrow \{\Phi(x) : x \in F\}$ 
     $\tilde{E} \leftarrow \left\{ \frac{e}{\|e\|_2} : e \in E \right\}$ 
     $z_{\text{ctx}} \leftarrow \Pi(\tilde{E})$ 
     $p_{\text{ctx}} \leftarrow f_{\text{ctx}}.\text{predict\_prob}(z_{\text{ctx}})$ 
     $\hat{c} \leftarrow \arg \max_c p_{\text{ctx}}(c)$ 
     $s_{\text{ctx}} \leftarrow \max_c p_{\text{ctx}}(c)$ 
    if  $s_{\text{ctx}} < \tau_{\text{ctx}}$  then
       $\hat{c} \leftarrow \text{LOW\_VIS}$ 
    // Activity pathway
     $x_{\text{act}} \leftarrow \Psi(w, F)$ 
     $p_{\text{act}} \leftarrow f_{\text{act}}.\text{predict\_prob}(x_{\text{act}})$ 
     $\hat{a} \leftarrow \arg \max_a p_{\text{act}}(a)$ 
     $s_{\text{act}} \leftarrow \max_a p_{\text{act}}(a)$ 
    if  $s_{\text{act}} < \tau_{\text{act}}$  then
       $\hat{a} \leftarrow \text{UNKNOWN}$ 
    Append:  $\langle \text{window\_id} = w, \text{start\_time} = \text{Start}(w), \text{end\_time} = \text{End}(w), \text{context} = \hat{c}, \text{context\_score} = s_{\text{ctx}}, \text{activity} = \hat{a}, \text{activity\_score} = s_{\text{act}} \rangle$  to  $\mathcal{T}(v)$ 
  for  $i \leftarrow 0$  to  $|\mathcal{T}(v)| - 1$  do
    if  $i = 0$  then
       $\mathcal{T}(v)[i].\text{context\_transition} \leftarrow \text{True}$ 
       $\mathcal{T}(v)[i].\text{activity\_transition} \leftarrow \text{True}$ 
    else
       $\mathcal{T}(v)[i].\text{context\_transition} \leftarrow$ 
         $(\mathcal{T}(v)[i].\text{context} \neq \mathcal{T}(v)[i-1].\text{context})$ 
       $\mathcal{T}(v)[i].\text{activity\_transition} \leftarrow$ 
         $(\mathcal{T}(v)[i].\text{activity} \neq \mathcal{T}(v)[i-1].\text{activity})$ 
  Return  $\{\mathcal{T}(v)\}_{v \in \mathcal{V}}$ 

```

---

APPENDIX B  
 ADDITIONAL CONFUSION ANALYSIS FIGURES

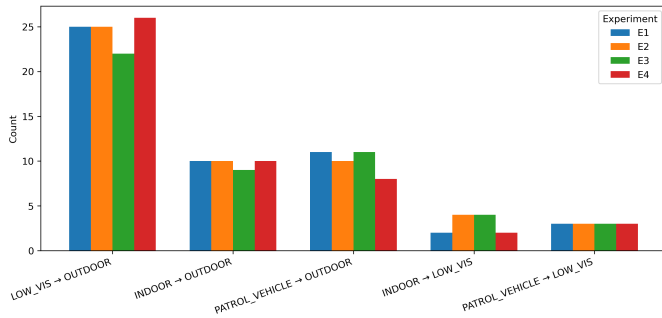


Fig. 8. Most frequent recurring context confusions across experiments.

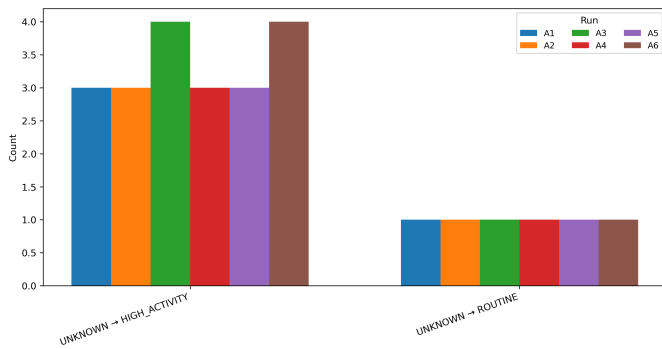


Fig. 9. Most frequent recurring activity confusions across CLIP-based runs, shown as counts per confusion type.

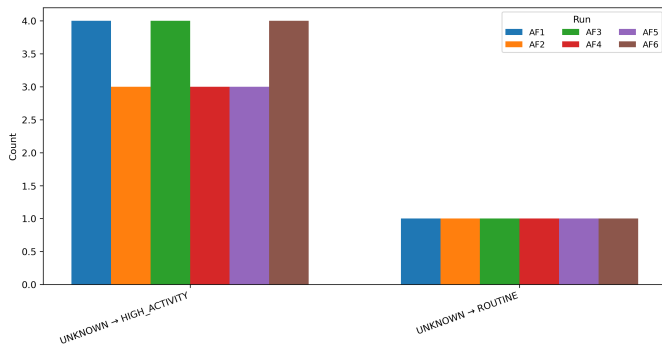


Fig. 10. Recurring activity confusions across fused runs, shown as counts per confusion type.